Proc. Natl. Acad. Sci. USA
Vol. 94, pp. 7103–7108, June 1997
Plant Biology

Purified vesicles of tobacco cell vacuolar and plasma membranes exhibit dramatically different water permeability and water channel activity

CHRISTOPHE MAUREL*†, FRÉDÉRIQUE TACNET‡, JOSETTE GÜCLÜ*, JEAN GUERN*, AND PIERRE RIPOCHE‡

*Institut des Sciences Végétales, Centre National de la Recherche Scientifique, F-91198 Gif-sur-Yvette Cedex, France; and ‡Biologie Cellulaire et Moléculaire, Commissariat à l'Energie Atomique/Saclay, F-91191 Gif-sur-Yvette Cedex, France

Communicated by Maarten J. Chrispeels, University of California at San Diego, La Jolla, CA, April 23, 1997 (received for review January 30, 1997)

ABSTRACT **The vacuolar membrane or tonoplast (TP) and the plasma membrane (PM) of tobacco suspension cells were purified by free-flow electrophoresis (FFE) and aqueous two-phase partitioning, with enrichment factors from a crude microsomal fraction of ≥4- to 5-fold and reduced contamination by other cellular membranes. For each purified fraction, the mean apparent diameter of membrane vesicles was determined by freeze-fracture electron microscopy, and the osmotic shrinking kinetics of the vesicles were characterized by stopped-flow light scattering. Osmotic water permeability coefficients (P_f) of 6.1 ± 0.2 and 7.6 ± 0.9 $\mu m \cdot s^{-1}$ were deduced for PM-enriched vesicles purified by FFE and phase partitioning, respectively. The associated activation energies (E_a; 13.7 ± 1.0 and 13.4 ± 1.4 $kcal \cdot mol^{-1}$, respectively) suggest that water transport in the purified PM occurs mostly by diffusion across the lipid matrix. In contrast, water transport in TP vesicles purified by FFE was characterized by (*i*) a 100-fold higher P_f of 690 ± 35 $\mu m \cdot s^{-1}$, (*ii*) a reduced E_a of 2.5 ± 1.3 $kcal \cdot mol^{-1}$, and (*iii*) a reversible inhibition by mercuric chloride, up to 83% at 1 mM. These results provide functional evidence for channel-mediated water transport in the TP, and more generally in a higher plant membrane. A high TP P_f suggests a role for the vacuole in buffering osmotic fluctuations occurring in the cytoplasm. Thus, the differential water permeabilities and water channel activities observed in the tobacco TP and PM point to an original osmoregulatory function for water channels in relation to the typical compartmentation of plant cells.**

In plants, the cell wall continuum and the cell-to-cell communications (plasmodesmata) provide privileged paths for water exchange and equilibration. Cellular membranes also critically control water transport in a variety of functions, including cell volume and turgor regulation and long-distance transport in nonvascular tissues (1). These functions involve the ability of membranes to transport or sequester osmotic solutes as well as their intrinsic permeability to water (1, 2). The presence in most plant cells of a large vacuole suggests that intra- and transcellular water exchange may depend on the permeability of two membranes in series, the plasma membrane (PM) and the vacuolar membrane or tonoplast (TP) (3, 4). Pressure probe measurements have brought about a better understanding of water relations in a variety of higher plant cell types (1, 5). However, this technique only provides access to the overall cell hydraulic conductivity that includes the water permeabilities of the PM and the TP plus those of the cell wall and the plasmodesmata. The individual water permeabilities of the two membranes thus remain to be determined in these cells (6).

The publication costs of this article were defrayed in part by page charge payment. This article must therefore be hereby marked "*advertisement*" in accordance with 18 U.S.C. §1734 solely to indicate this fact.

The possible existence of water-transporting pores or water channels in membranes of higher plants was discussed nearly 40 years ago (7, 8). However, experimental approaches to the molecular mechanisms of membrane water permeability in these organisms have been rare until recently (6), and the diffusion of water molecules across the lipid matrix was generally considered sufficient to account for transmembrane water exchange. Yet the existence of water channels had been demonstrated in certain biological membranes (for reviews, see refs. 2 and 9). Typical features of these membranes include a ratio of osmotic-to-diffusional water permeabilities (P_f/P_d) greater than unity and a low Arrhenius activation energy (E_a < 6 $kcal \cdot mol^{-1}$) for water transport and its reversible inhibition by mercury sulfhydryl reagents (2, 9). With use of these criteria, functional evidence for water channels was obtained for the giant internodal cells of the Characeae (10, 11), but similar experiments were never done with higher plants. Recently, a class of water channel proteins named aquaporins has been identified in a wide variety of living organisms, including higher plants (6, 9, 12). Plant aquaporins have been localized in the TP and the PM, where they define the tonoplast intrinsic protein (TIP) and plasma membrane intrinsic protein (PIP) subfamilies (6, 12). However, plant aquaporins have been functionally characterized after expression in *Xenopus* oocytes but not in their native membranes (6).

Stopped-flow spectrophotometry enables accurate measurements of osmotic water permeability in purified membrane vesicles (13). This technique has proved extremely useful in dissecting the mechanisms and regulation of water transport in animal cellular membranes (13) but has been scarcely used in plants (§, 14). In the present work, we apply this technique to investigate the characteristics of water transport across the TP and PM of plant cells. The numerous aquaporin isoforms present in plants exhibit complex developmental expression patterns (6). To avoid problems caused by the presence of numerous aquaporins in different cell types, we used exponentially growing tobacco suspension cells, which are ontogenically quite uniform, for the isolation and characterization of the water permeability of TP and PM vesicles.

MATERIALS AND METHODS

Cells. Suspension-cultured tobacco (*Nicotiana tabacum* cv. Xanthi) cells were maintained in B5 Gamborg medium containing 1 μM 2,4-dichlorophenoxyacetic acid and 60 nM

Abbreviations: E_a, Arrhenius activation energy; FFE, free-flow electrophoresis; P_f, osmotic water permeability coefficient; PM, plasma membrane; TP, tonoplast.

†To whom reprint requests should be addressed at: Institut des Sciences Végétales Bâtiment 22, Centre National de la Recherche Scientifique, F-91198 Gif-sur-Yvette Cedex, France. e-mail: maurel@cactus.isv.cnrs-gif.fr.

§Niemietz, C. & Tyerman, S. D. (1995) 10th International Workshop on Plant Membrane Biology, Aug. 6–11, Regensburg, Germany, abstr. C76.

kinetin in the light at 26°C and were subcultured every 7 days at a density of 15–30 mg (fresh weight)·ml^{-1}. Exponentially growing cells were used 4–5 days after transfer.

Membrane Purification. Microsomal membranes were prepared as described (15), resuspended in a free-flow electrophoresis (FFE) chamber buffer (300 mM sucrose/9 mM KCl/10 μM $MgCl_2$/10 mM Tris/10 mM boric acid, pH 8.3), and separated by continuous FFE (16) at 4°C and 1,050-V constant voltage (current intensity = 120–150 mA) in a Elphor VaP 22 unit (Bender and Hobein, Münich, Germany). Sample was injected at a rate of 7–8 mg of protein·h^{-1} in a buffer flow of 3.5 ml·h^{-1} per fraction. The separation profile was monitored by absorbance at 280 nm, and fractions were pooled as exemplified in Fig. 1*A*. In particular, the shoulders migrating the most toward the anode and the cathode were taken as TP- and PM-enriched fractions, respectively (see *Results*). Membranes were collected by centrifugation at 150,000 × *g* for 30 min, resuspended at about 10 mg of protein·ml^{-1} in 330 mM sucrose/5 mM KCl/1 mM DTT/0.5 mg·ml^{-1} leupeptin/10 mM Mes–Tris, pH 6.0; frozen in liquid nitrogen; and stored at −80°C until use. Alternatively, the PM was purified essentially as described (15) by partitioning the microsomal membrane fraction in an aqueous polyethylene glycol/dextran two-phase system with 5 mM KCl and 6.6% (wt/wt) of each polymer. FFE membrane purification from 100–130 g fresh weight yielded TP- and PM-enriched fractions of 0.9–1.3 mg and 1.0–1.4 mg of protein, respectively, whereas PM-enriched fractions obtained by two-phase partition contained 0.6–0.7 mg of protein. Marker enzyme assays (17) and freeze-fracture electron microscopy (18) were performed as previously described.

Water Permeability Measurements. Water transport measurements were performed at 20°C or at the indicated temperature essentially as described (18). Briefly, purified membrane vesicles were diluted to 70–250 μg of protein·ml^{-1} in buffer A (50 mM mannitol/5 mM KCl/1 mM $MgCl_2$/20 mM Mes–Tris, pH 6.0). The associated hypoosmotic shock induces a transient opening of the vesicles and their equilibration with buffer A. This allows further P_f measurements at reduced external osmolality and a better resolution of the shrinking kinetics (see *Results*). For this, vesicles in buffer A were mixed in an SFM3 stopped-flow spectrophotometer (Biologic, Claix, France) to a similar solution but complemented with mannitol. This resulted in exposure, with a dead time of <2 ms, to an inwardly directed osmotic gradient of, unless otherwise indicated, 80 milliosmolal (mosmol)·kg^{-1} H_2O. The intensity of 90° scattered light at λ_{ex} = 510 nm was recorded at an acquisition rate of 200-2000 Hz. Data from 5–10 time courses were averaged and fitted to single or multi-exponential functions by using the Simplex procedure of a BIOKINE software (Biologic). The osmotic water permeability coefficient (P_f) was calculated according to the following equation (19): $P_f = k \cdot V_0/S \cdot V_w \cdot C_{out}$, where k is the fitted exponential rate constant, V_0 is the initial mean vesicle volume, S is the mean vesicle surface, V_w is the molar volume of water, and C_{out} is the external osmolality. Solution osmolalities were measured on a vapor pressure osmometer (Wescor, Logan, UT).

RESULTS

Purification of TP and PM from Tobacco Suspension Cells. FFE allows the purification of plant TP and PM, under identical conditions, from the same cell homogenate (16). A crude microsomal fraction from tobacco suspension cells was resolved by FFE and yielded a typical separation profile with a major peak and minor peaks on either side (Fig. 1*A*). Six membrane subpools (pooled fractions A–F) were determined from this profile and assayed for marker enzyme activities (17). The TP markers, pyrophosphatase and NO_3^--inhibited ATPase, showed the highest specific activities in the most electronegative fractions (anodic side), whereas the PM markers,

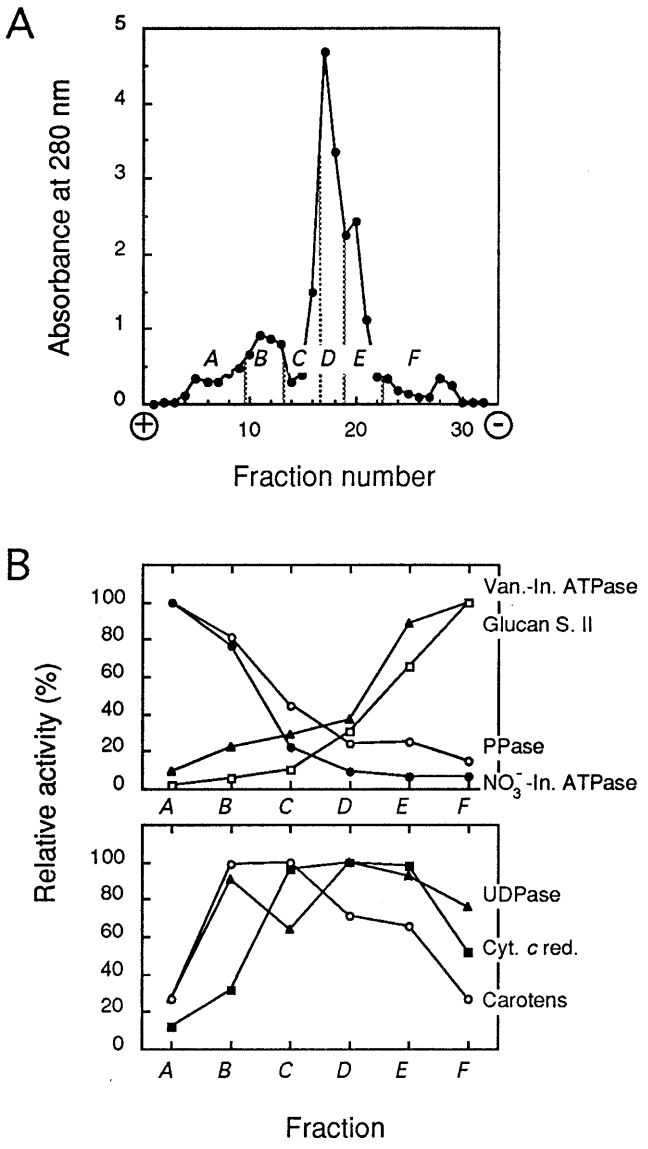

FIG. 1. FFE separation of tobacco cell membranes. (*A*) Representative separation profile determined by absorbance at 280 nm. A–F, pooled fractions. (*B*) Membrane marker activities in the A–F membrane fractions expressed as the percentage of the highest specific activity detected in either fraction. Mean data from four independent membrane separations and enzymatic activity measurements are shown. Specific activities at 37°C (100%; in millimoles per hour per milligram of protein) were as follows: vanadate-inhibited ATPase (Van.-In. ATPase; ▲), 9.25; glucan synthase II (Glucan S. II; □), 4.57; pyrophosphatase (PPase; ○), 9.32; NO_3^--inhibited ATPase (NO_3^--In. ATPase; ●), 2.37; latent uridine-5′-diphosphatase (UDPase; ▲), 8.50; NADPH-cytochrome *c* reductase (Cyt. *c* red.; ■), 25.20; carotenoids (Carotens; ○), 100% represents 3.07 mg per mg of protein.

glucan synthase II and vanadate-inhibited ATPase, accumulated in fractions migrating closest to the cathode (Fig. 1*B*). More specifically, fraction A displayed an enrichment factor from the initial microsomal fraction of 5.1 (± 0.3; n = 4) in NO_3^--inhibited ATPase activity, whereas fraction F was enriched 2.2-fold (± 0.2; n = 4) in vanadate-inhibited ATPase activity. In addition, antigens related to the E-subunit of a barley vacuolar H^+-ATPase were immunodetected in fraction A but barely in fraction F. Antibodies directed to a tobacco PM H^+-ATPase specifically reacted with fraction F (data not shown). Altogether, these results show that the TP and PM of tobacco cells can be enriched in fractions A and F, respectively, and are, in these fractions, largely free of contamination each from the other. Latent uridine-5′-diphosphatase, cytochrome

c oxidase (not shown), NADPH-cytochrome *c* reductase, and carotenoids were used as markers for the Golgi, mitochondria, endoplasmic reticulum, and plastid membranes, respectively (17). Fig. 1*B* shows that TP-enriched fraction A was clearly depleted in these markers. In contrast, PM-enriched fraction F appeared to be contaminated by Golgi and endoplasmic reticulum membranes.

To obtain preparations of tobacco cell PM of higher purity, we used the aqueous two-phase partition technique (17). An upper phase was obtained with an enrichment from the microsomal fraction of 4- to 5-fold in vanadate-inhibited ATPase activity (not shown). This PM-enriched fraction also displayed limited contamination by other cell membranes, with enrichment factors in cytochrome *c* oxidase, NADPH-cytochrome *c* reductase, and UDPase of <0.25 (unpublished data and ref. 15).

Purified membrane fractions were visualized by freeze-fracture electron microscopy. The PM- and TP-enriched fractions obtained by FFE mostly appeared as spherical vesicles (not shown) with a mean apparent diameter of 154 ± 6 nm (n = 131) and 320 ± 16 nm (n = 133), respectively. Two-phase partitioning yielded PM-enriched vesicles of 133 ± 6 nm (n = 144) in diameter.

Osmotically Induced Changes in PM- and TP-Enriched Vesicle Volume. PM- and TP-enriched vesicles prepared by FFE were exposed in a stopped-flow apparatus to an inwardly directed 82 mosmol·kg^{-1} mannitol gradient. Fig. 2 shows that this resulted in a time-dependent increase in scattered light intensity that was completed in 5–6 s with PM-enriched vesicles but occurred much faster (in 0.1–0.2 s) with TP-enriched vesicles.

The light scattering response of PM- and TP-enriched vesicles was analyzed in more detail to assess their osmotic behavior in this assay. No time-dependent change in light signal was observed after exposure of the vesicles to an isoosmotic medium. Furthermore, the amplitude of change in light scattering increased in both types of vesicles with the size of the imposed inwardly directed osmotic gradient and was proportional to the ratio of initial extra- to intravesicular osmolalities (Fig. 3*A*). This ratio also corresponds to the ratio of initial to final vesicle volumes expected after an osmotically induced water efflux. These results are consistent with the double hypothesis that (*i*) tobacco TP- and PM-enriched vesicles exhibit the generally observed inverse relationship between scattered light intensity and vesicle volume (19), and (*ii*) the increase in light scattering reflected the shrinkage of these vesicles because of osmotic water efflux.

The light scattering kinetics of PM- and TP-enriched vesicles could be fitted to monoexponential functions (Fig. 2) whose rate constants were proportional to the extravesicular osmolality (Fig. 3*B*). These features conform to the theoretical analysis developed by van Heeswijk and van Os (19) to describe the scattered light signal associated to the osmotic shrinking of membrane vesicles. We also observed that after the first increase, the optical signal of tobacco PM-enriched and, to a lesser extent, that of TP-enriched vesicles, was fairly constant for several seconds. This suggested that, during this interval and despite its strong concentration gradient, mannitol did not penetrate or penetrated at a reduced rate into the shrunken vesicles. Altogether, these results show that at least a fraction of the two types of purified membrane vesicles were sealed, behaved as proper osmometers, and were thus suited for water permeability measurements.

Water Permeabilities of the PM- and TP-Enriched Vesicles. The osmotic water permeability coefficients (P_f) of purified membrane vesicles were calculated from their osmotic shrinking kinetics and their volume-to-surface ratio, as estimated by freeze-fracture electron microscopy (Table 1). A P_f value of 6.1 ± 0.2 μm·s^{-1} at 20°C was deduced for PM-enriched vesicles prepared by FFE. PM vesicles purified by two-phase partition displayed essentially similar stopped-flow behavior and a P_f of 7.6 ± 0.9 μm·s^{-1}. In contrast, and as reflected by much faster shrinking kinetics despite a larger size, the TP-enriched ves-

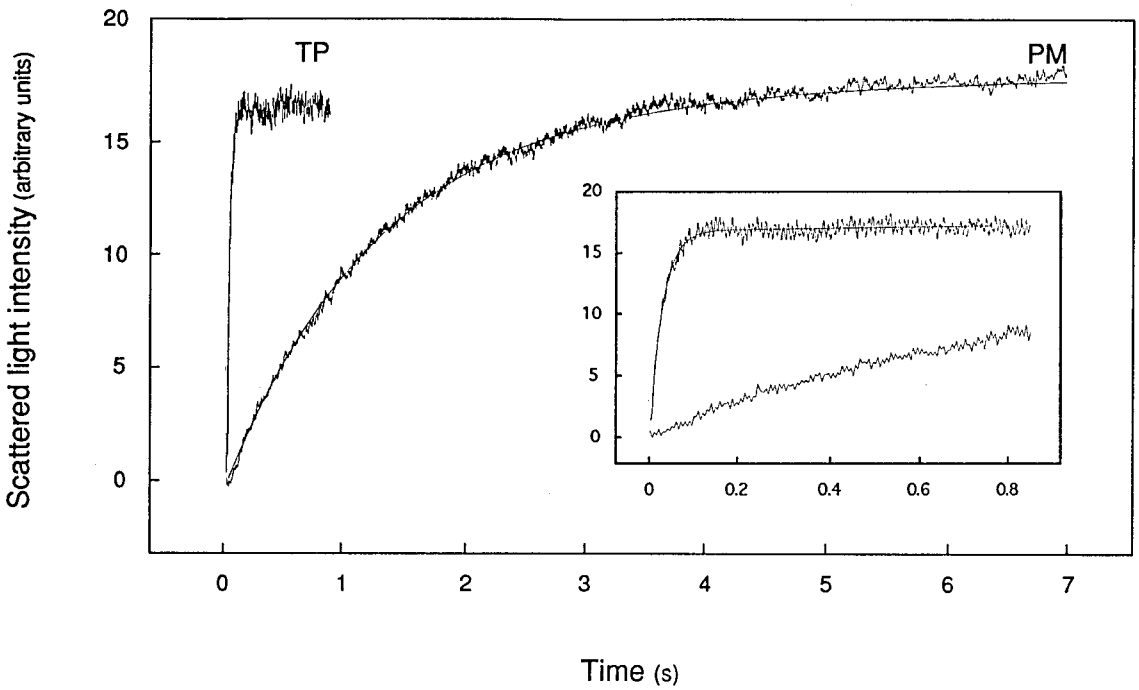

FIG. 2. Time course of increased scattered light intensity in PM- and TP-enriched membrane vesicles. Membranes were purified by FFE, resuspended in 50 mM mannitol/5 mM KCl/1 mM $MgCl_2$/20 mM Mes–Tris, pH 6.0 (C_{in} = 92 mosmol·kg^{-1}), and submitted in a stopped-flow apparatus (t = 20.0°C) to an 82 mosmol·kg^{-1} inwardly directed mannitol gradient (C_{out} = 174 mosmol·kg^{-1}) at time 0. The figure shows for both types of membrane preparations a typical experiment with the average trace of five to seven individual shots and the fitted monoexponential function. (*Inset*) Same recordings on a reduced time scale. The monoexponential rate constant (k) and the deduced osmotic water permeability (P_f) were as follows: PM, k = 0.77 s^{-1}, P_f = 6.2 μm·s^{-1}; TP, k = 34.7 s^{-1}, P_f = 682 μm·s^{-1}.

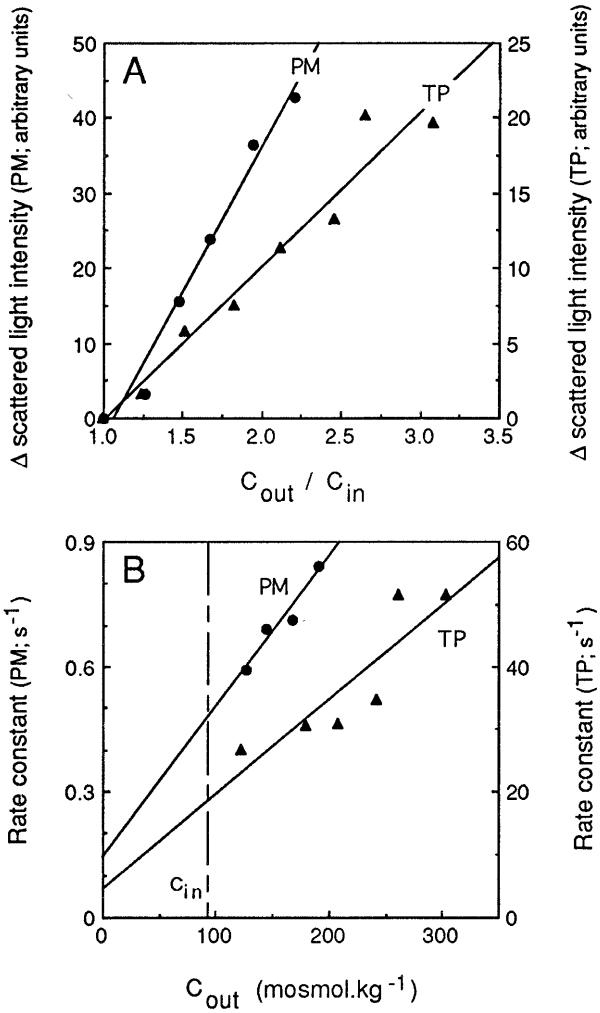

FIG. 3. Effects of external osmolality on the time-dependent changes in scattered light intensity. PM- and TP-enriched membrane vesicles were purified by FFE, resuspended in 50 mM mannitol/5 mM KCl/1 mM $MgCl_2$/20 mM Mes–Tris, pH 6.0 (C_{in}= 92 mosmol·kg^{-1}), and exposed, as exemplified in Fig. 2, to external media of different osmolalities (C_{out}) obtained by addition of mannitol to the vesicle suspension buffer. (*A*) Effects of the size of the imposed osmotic gradient, expressed as C_{out}/C_{in}, on the maximal amplitude of change in scattered light intensity. (*B*) Effects of C_{out} on the fitted monoexponential rate constant. Straight lines were fitted to the experimental data by a least-squares protocol. Note that data for PM and TP are plotted along different ordinates.

icles exhibited a P_f of 690 ± 35 μm·s^{-1} at 20°C and were thus 100-fold more permeable to water than their PM counterparts.

Features of Water Permeation Through the PM- and TP-Enriched Vesicles. The temperature dependence of P_f in TP- and PM-enriched vesicles was determined between 6°C and 36°C and is shown as an Arrhenius plot in Fig. 4. A linear fit to the data indicated an apparent activation energy (E_a) of 2.5 ± 1.3 kcal·mol^{-1} for water transport in TP-enriched vesicles. This suggests that a path for facilitated diffusion of water (i.e., aqueous pores) predominates in this membrane (2). In contrast, E_a values of 13.7 ± 1.0 and 13.4 ± 1.4 kcal·mol^{-1} were calculated for water transport in PM-enriched vesicles prepared by FFE or two-phase partition, respectively (Table 1). The range of these values suggests that water molecules permeate the purified PM mostly by a lipid pathway (2). However, in half of the PM vesicle preparations obtained by either FFE or two-phase partition, an upward deflection in the Arrhenius curve was observed for temperatures below 11–15°C (Fig. 4). This discontinuity suggested that a water transport mechanism with a lower E_a (<6 kcal·mol^{-1}) can become predominant at low temperatures in the vesicle population.

The existence of water-transporting pores in the purified TP was further investigated by using mercuric chloride ($HgCl_2$), a reversible blocker of most aquaporin water channels (6, 9, 20). The preincubation for 5 min of TP-enriched vesicles with $HgCl_2$ concentrations of ≥0.3 mM resulted in a marked inhibition of osmotic water transport (Fig. 5*A*). P_f at 20°C was

Table 1. Characteristics of osmotic water transport in membrane vesicles purified from tobacco suspension cells

Membrane fraction	Isolation procedure	P_f, μm·s^{-1}	E_a, kcal·mol^{-1}
PM-enriched	2-PP	7.6 ± 0.9 (5)	13.4 ± 1.4 (2) (1)*
	FFE	6.1 ± 0.2 (6)	13.7 ± 1.0 (4) (2)*
TP-enriched	FFE	690 ± 35 (7)	2.5 ± 1.3 (3)

Osmotic water permeability coefficients (P_f) at 20°C and Arrhenius activation energies (E_a) are indicated ±SEM with the number of independent membrane preparations in parentheses. 2-PP, two-phase partition.

*Values in the second set of parentheses indicate the number of PM preparations with a nonlinear Arrhenius curve.

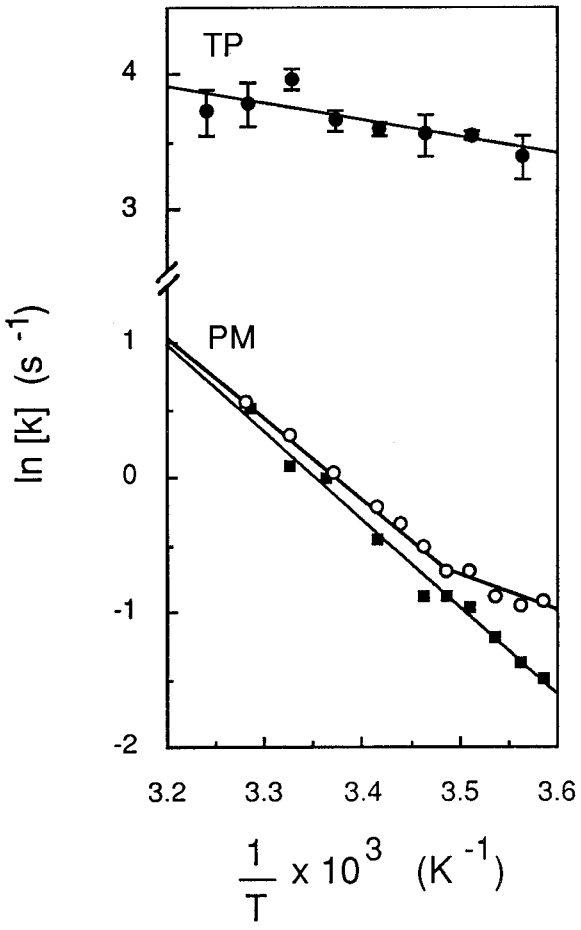

FIG. 4. Temperature dependence of osmotic water transport in PM- and TP-enriched vesicles. Exponential rate constants (k) of vesicle osmotic shrinking were determined at the indicated temperature (T), as exemplified in Fig. 2. Data were plotted in an Arrhenius representation and activation energy (E_a) values were deduced from the slope of lines fitted by linear regression to the experimental data. For TP (●), mean values from measurements of three independent membrane preparations are shown, and E_a = 2.5 ± 1.3 kcal·mol^{-1}. For PM (○ and ■), data from two individual FFE membrane preparations are shown. ■, E_a = 12.5 kcal·mol^{-1}; ○, for $10^3/T \leq 3.487$ K^{-1} ($t \geq 13.8$°C), E_a = 12.0 kcal·mol^{-1}; for $10^3/T \geq 3.487$ K^{-1} ($t \leq 13.8$°C), E_a = 5.4 kcal·mol^{-1}.

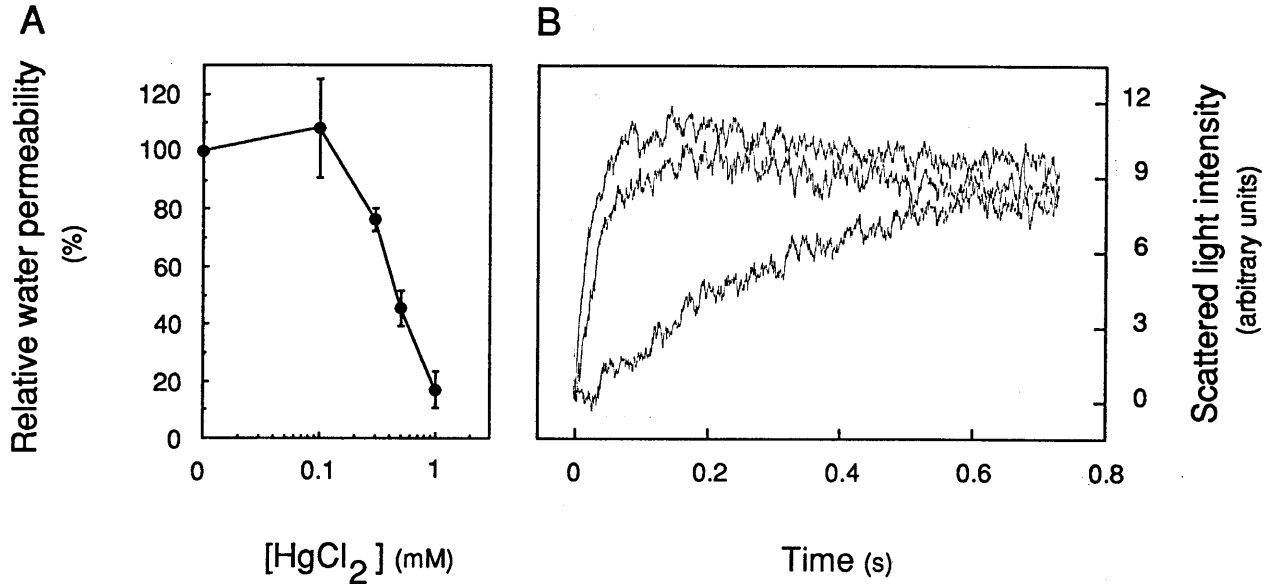

FIG. 5. Mercury inhibition of osmotic water transport in TP-enriched vesicles. (*A*) Dose dependence of inhibition. Vesicles were preincubated at room temperature for 5 min at the indicated $HgCl_2$ concentration; P_f values were measured at 20°C in the presence of an 80 mosmol·kg^{-1} mannitol gradient and were reported to the P_f value measured in control untreated vesicles. (*B*) Reversion of mercury inhibition by a reducing agent. Top curve, untreated control (k = 43.9 s^{-1}); middle curve, after exposure for 5 min to 1 mM $HgCl_2$ and for 15 min with the addition of 10 mM 2-mercaptoethanol (k = 31.5 s^{-1}); bottom curve, after exposure for 5 min to 1 mM $HgCl_2$ (k = 4.2 s^{-1}). Note that the slowly decaying plateau of the top and middle curves may indicate a slight permeability of the TP vesicles to mannitol in this experiment.

reduced to 17 ± 6% (n = 3) of its initial value in the presence of 1 mM $HgCl_2$. The addition to the inhibition mixture of a reducing agent (10 mM 2-mercaptoethanol for 15 min) reversed most of these effects and resulted in a P_f value 70 ± 4% (n = 2) that of nontreated membrane vesicles (Fig. 5*B*). These results support the idea that water channels can account for most of the water permeability of TP-enriched vesicles. In contrast to its effects on TP vesicles, $HgCl_2$ did not inhibit the P_f of PM-enriched vesicles at 20°C or 13°C.

DISCUSSION

In contrast to techniques previously used in higher plants, stopped-flow spectrophotometry allows accurate osmotic water permeability measurements in defined subcellular membranes. This technique must, however, be combined with efficient membrane purification procedures. In the present work, we used FFE and aqueous two-phase partitioning and obtained membrane fractions that, according to the presence of enzymatic markers, were enriched ≥4- to 5-fold in PM and TP vesicles. Functional evidence also supports the purity of these fractions. First, the osmotic shrinking kinetics of both types of purified membranes could be represented by single exponential functions. This indicates that each of these fractions contained a functionally homogenous vesicle population, which we associate with the PM and the TP, the predominant membranes in these vesicle fractions. Second, similar transport characteristics were observed after PM purification by either FFE or two-phase partitioning. Third, the TP- and PM-enriched fractions exhibited completely different osmotic behavior in accordance with their low levels of biochemical cross-contamination. We could thus measure for the tobacco TP a P_f that ranks among the highest values reported in plant and animal membranes (6, 9). In contrast, the tobacco PM was moderately permeable to water, with a 100-fold lower P_f. Such differential water permeability in two subcellular membranes prepared in parallel from the same cell is undoubtedly the most striking result of the present work.

Comparative measurements of the plant TP and PM water permeabilities have been attempted in only a few previous studies (3, 21, 22). Kiyosawa and Tazawa (22) proposed that in *Chara australis* internodal cells, the water permeability of the TP is much higher than that of the PM because selective disruption of the TP by an intracellular perfusion procedure did not change the transcellular osmotic water permeability. These results are at variance with those obtained in *Chara corallina* cells using nondestructive pressure probe measurements (21, 23). A compartmental analysis of turgor pressure relaxations indicated high P_f values for both the PM and the TP, in the range of 200–400 μm·s^{-1} (21, 23). To our knowledge, the only P_f estimate of a higher plant TP was obtained by Url (3) in onion epidermal cells. Plasmometric measurements indicated a reduced P_f for the plasmolyzed protoplasts, in the range of 10 μm·s^{-1}, and a 40- to 100-fold higher permeability for vacuoles isolated by the eventual disruption of protoplasts after repetitive osmotic challenge. These and our results point to a same difference in TP and PM water permeability. However, the reliability of the plasmometric method is questionable because of unstirred layer effects and limited diffusion of the osmoticum in the cell wall (6). The present work provides thus a novel contribution to the long-standing question of the site(s) of penetration resistance to water in plant cells (3, 4), and it will be of interest to investigate further whether a water permeability higher in the TP than in the PM is a common feature of higher plant cells.

The long-observed variability in water permeability of plant cells or membranes has been tentatively explained by methodological uncertainties or differences in lipid membrane composition (24). The plant PM and TP have indeed different lipid profiles (25, 26), but the relevance of these to the individual P_f of the two membranes remains poorly understood (14). In contrast to those ideas, the low E_a (<6 kcal·mol^{-1}) and the reversible inhibition by mercury of water transport in tobacco TP vesicles show that functional water channels contribute >80% to the membrane P_f and, as a consequence, might account for its extremely high permeability. The present work thus provides the first (to our knowledge) complete functional (biophysical) evidence for water channels in a higher plant cell membrane. The contribution of a class of water channels, the PIP aquaporins, to water transport across

plant membranes has also been suggested by the observation that *Arabidopsis* leaf protoplasts containing a PIP1b aquaporin antisense transgene showed delayed bursting after a hypoosmotic challenge (27). In tobacco, the molecular identity of the TP water channels remains to be determined, but preliminary evidence indicates that suspension cells express high mRNA levels for TIP homologs, some of which have been shown to function as aquaporins (28–30). In contrast to the TP, the tobacco cell PM exhibited a low P_f and a high E_a for water transport, indicating a predominant lipid solubility–diffusion mechanism for water permeation across this membrane. The nonlinearity of some of the PM Arrhenius curves remains unexplained and could reflect either a minor contamination of the PM by other membranes with a lower E_a or a low density of functional water channels in the PM itself, both of which become predominant at low temperatures (31). There is indeed evidence for functional aquaporins in the PM of *Arabidopsis* (27). Nevertheless, our results show that distinct mechanisms of water permeation can operate in the TP and the PM of plant cells. Because of possible artifacts caused by the vesicle preparation methods, it remains to be determined whether the P_f configuration described here for the TP and PM occurs in living tobacco cells. Regulatory processes such as the posttranslational modification of water channel proteins (29, 32) or their regulated trafficking (20) may also operate in the TP and possibly in the PM of these cells.

In plants, the vacuolar apparatus occupies most of the cell interior and a high TP water permeability might provide the cell with a reduced resistance to transcellular water flow (12). The plant cell configuration also requires water to be transported in and out of the vacuole(s) for any change in cell volume. During these processes, the cytoplasm that is reduced to a thin layer between the TP and the PM will be sensitive to any differential flow of water occurring across the two membranes. It appears that nonlimiting water transport at the TP may allow the plant cell to use efficiently the vacuolar space for buffering osmotic fluctuations that occur in the cytoplasm (28). In particular, and as confirmed by simulations of water transport dynamics in a three-compartment model of plant cells (unpublished work and ref. 33), a P_f higher in the TP than in the PM would avoid the transient collapse or swelling of the cytoplasm, in case of a sudden osmotic stress originating from the extracellular space. In agreement with this concept is the recent observation that aquaporins in the PM of *Arabidopsis* leaf cells accumulate in plasmalemmasomes that protrude deep into the vacuole (34). This might provide another mechanism for optimizing water exchange between the vacuole and the apoplast, with minor osmotic perturbation in the cytoplasm.

The specific regulation of P_f in subcellular membranes has been clearly established in the epithelia of the kidney collecting duct, where vasopressin fine-tunes transcellular water flow (reabsorption) (20). However, the typical compartmentation of plant cells with a predominant vacuole raises specific constraints to intra- and transcellular water transport. The differential regulation of water permeability observed in the plant TP and PM might respond to these constraints and suggests an original function for membrane water channels in cell osmoregulation.

The assistance of Renée Gobin in freeze fracture electron microscopy is gratefully acknowledged. We also thank Hervé Canut for helpful advice in FFE separation; Marc Boutry and Karl-Josef Dietz for antibodies directed against a tobacco PM H^+-ATPase and a barley vacuolar H^+-ATPase, respectively; and Hélène Barbier-Brygoo and Claire Lurin for critical reading of the manuscript. This research was supported by the Centre National de la Recherche Scientifique (UPR0040), the Ministère de l'Enseignement Supérieur et de la Recherche (MESR-CNRS Réponses adaptatives aux stress environnementaux, Réseau No. 6), and the Commissariat à l'Energie Atomique (Direction des Sciences du Vivant, segment 28).

1. Steudle, E. (1994) in *Flux Control in Biological Systems: From Enzymes to Populations and Ecosystems*, ed. Schultze, E. D. (Academic, San Diego), pp. 237–299.
2. Finkelstein, A. (1987) *Distinguished Lecture Series of the Society of General Physiologists* (Wiley, New York), Vol. 4, pp. 1–228.
3. Url, W. G. (1971) *Protoplasma* **72,** 427–447.
4. Collander, R. (1959) in *Plant Physiology: A Treatise*, ed. Steward, F. C. (Academic, New York and London), pp. 3–102.
5. Zimmermann, U. (1989) *Methods Enzymol.* **174,** 338–366.
6. Maurel, C. (1997) *Annu. Rev. Plant Physiol. Plant Mol. Biol.* **48,** 399–429.
7. Dainty, J. (1963) *Adv. Bot. Res.* **1,** 279–326.
8. Ray, P. M. (1960) *Plant Physiol.* **35,** 783–795.
9. van Os, C. H., Deen, P. M. T. & Dempster, J. A. (1994) *Biochim. Biophys. Acta* **1197,** 291–309.
10. Wayne, R. & Tazawa, M. (1990) *J. Membr. Biol.* **116,** 31–39.
11. Henzler, T. & Steudle, E. (1995) *J. Exp. Bot.* **46,** 199–209.
12. Chrispeels, M. J. & Maurel, C. (1994) *Plant Physiol.* **105,** 9–13.
13. Verkman, A. S. (1995) *J. Membr. Biol.* **148,** 99–110.
14. Schuler, I., Milon, A., Nakatani, Y., Ourisson, G., Albrecht, A.-M., Benveniste, P. & Hartmann, M.-A. (1991) *Proc. Natl. Acad. Sci. USA* **88,** 6926–6930.
15. Mathieu, Y., Sanchez, F. J., Droillard, M.-J., Lapous, D., Laurière, C. & Guern, J. (1996) *Plant Physiol. Biochem.* **34,** 399–408.
16. Sandelius, A. S., Penel, C., Auderset, G., Brightman, A., Millard, M. & Morré, D. J. (1986) *Plant Physiol.* **81,** 177–185.
17. Briskin, D. P., Leonard, R. T. & Hodges, T. K. (1987) *Methods Enzymol.* **148,** 542–558.
18. Laizé, V., Rousselet, G., Verbavatz, J.-M., Berthonaud, V., Gobin, R., Roudier, N., Abrami, L., Ripoche, P. & Tacnet, F. (1995) *FEBS Lett.* **373,** 269–274.
19. van Heeswijk, M. P. E. & van Os, C. H. (1986) *J. Membr. Biol.* **92,** 183–193.
20. King, L. S. & Agre, P. (1996) *Annu. Rev. Physiol.* **58,** 619–648.
21. Wendler, S. & Zimmermann, U. (1985) *J. Membr. Biol.* **85,** 133–142.
22. Kiyosawa, K. & Tazawa, M. (1977) *J. Membr. Biol.* **37,** 157–166.
23. Wendler, S. & Zimmermann, U. (1985) *J. Membr. Biol.* **85,** 121–132.
24. Steudle, E. (1989) *Methods Enzymol.* **174,** 183–225.
25. Yoshida, S. & Uemura, M. (1986) *Plant Physiol.* **82,** 807–812.
26. Brown, D. J. & DuPont, F. M. (1989) *Plant Physiol.* **90,** 955–961.
27. Kaldenhoff, R., Kölling, A., Meyers, J., Karmann, U., Ruppel, G. & Richter, G. (1995) *Plant J.* **7,** 87–95.
28. Maurel, C., Reizer, J., Schroeder, J. I. & Chrispeels, M. J. (1993) *EMBO J.* **12,** 2241–2247.
29. Maurel, C., Kado, R. T., Guern, J. & Chrispeels, M. J. (1995) *EMBO J.* **14,** 3028–3035.
30. Daniels, M. J., Chaumont, F., Mirkov, T. E. & Chrispeels, M. J. (1996) *Plant Cell* **8,** 587–599.
31. Meyer, M. M. & Verkman, A. S. (1987) *J. Membr. Biol.* **96,** 107–119.
32. Kuwahara, M., Fushimi, K., Terada, Y., Bai, L., Marumo, F. & Sasaki, S. (1995) *J. Biol. Chem.* **270,** 10384–10387.
33. Tyree, M. T. (1980) in *Plant Membrane Transport: Current Conceptual Issues*, eds. Spanswick, R. M., Lucas, W. J. & Dainty, J. (Elsevier/North–Holland, Amsterdam), pp. 459–460.
34. Robinson, D. G., Sieber, H., Kammerloher, W. & Schäffner, A. R. (1996) *Plant Physiol.* **111,** 645–649.